Synthesis of defined oligohyaluronates-decorated liposomes and interaction with lung cancer cells

Maria Emilia Cano, David Lesur, Valeria Bincoletto, Elena Gazzano, Barbara Stella, Chiara Riganti, Silvia Arpicco, José Kovensky

Synthesis of defined oligohyaluronates-decorated liposomes and interaction with lung cancer cells

Maria Emilia Cano [a], David Lesur [a], Valeria Bincoletto [b], Elena Gazzano [c], Barbara Stella [b], Chiara Riganti [c], Silvia Arpicco [b,*], José Kovensky [a,*]

[a] *Laboratoire de Glycochimie, des Antimicrobiens et des Agroressources CNRS UMR 7378, Université de Picardie Jules Verne, 33 rue Saint Leu, 80039 Amiens, France*

[b] *Department of Drug Science and Technology, University of Torino, Via Giuria 9, 10125 Torino, Italy*

[c] *Department of Oncology, University of Torino, Via Santena 5/bis, 10126 Torino, Italy*

*Corresponding authors: silvia.arpicco@unito.it; jose.kovensky@u-picardie.fr

In this work hyaluronic acid (HA) oligosaccharides with degree of polymerization (DP) 4, 6 and 8, obtained by enzymatic depolymerization of HA, were conjugated to a PEG-phospholipid moiety. The products (HA-DP4, HA-DP6 and HA-DP8) were used to prepare decorated liposomes. The cellular uptake of HA-DP4, HA-DP6 and HA-DP8-decorated fluorescently labelled liposomes was significantly higher (12 to 14-fold) in lung cancer cell lines with high CD44 expression than in those with low CD44 expression, suggesting a receptor-mediated entry of HA-conjugated formulations. Competition assays showed that the uptake followed this rank order: HA-DP8>HA-DP6>HA-DP4 liposomes. Moreover, they are capable of a faster interaction with CD44, followed by phagocytosis, than HA liposomes obtained from HA of higher molecular weight (4800 and 14800 Da). HA-DP4, HA-DP6 and HA-DP8-liposomes did not show cytotoxicity or inflammatory effects. Overall, we propose our new HA-DP oligosaccharides as biocompatible and effective tools for a potential drug delivery to CD44-positive cells.

Keywords: Hyaluronic acid; oligosaccharides; liposomes; HA-CD44 interaction

1. Introduction

Hyaluronic acid (HA) is a widely distributed extracellular matrix polysaccharide of the glycosaminoglycan family. It is a polymer of high molecular weight composed of alternating glucuronic acid (GlcA) and *N*-acetylglucosamine (GlcNAc) units forming a repeating sequence of the disaccharide β-D-GlcA-(1→3)-β-D-GlcNAc-(1→4). This biomolecule is involved in the regulation of inflammation, tumor development and healing processes through its interaction with different proteins (Fuster & Esko, 2005; Toole, 2004).

HA is considered as a key biomarker of specific cancers, because CD44, the main receptor of HA at the cell surface, is overexpressed on different solid (colon, ovarian, breast, lung) tumors and leukemias. The binding of HA to CD44 modulates the regulation and the proliferation of cancer cells. Recently, it has been reported that the repeating sequence of HA provides multiple binding sites for CD44 binding, inducing CD44 clustering, an event related to tumor progression and inflammation processes (Yang et al., 2012).

This binding has prompted researchers to use HA-phospholipid conjugates to construct liposomes able to target tumor cells through the CD44 receptor. In previous works, it has been shown that such liposomes can successfully bind to cells, and if they are loaded with anticancer drugs as gemcitabine or doxorubicin derivatives, they can be internalized and delivered efficiently. (Arpicco et al., 2013; Dalla Pozza et al., 2013; Gazzano et al., 2019; Marengo et al., 2019).

Like other polymers, macromolecular HA is not homogeneous: indeed, it is composed of multiple chains of different length, with an average molecular weight of about 10^6 Da. Oligosaccharides of lower molecular weight that can be obtained by chemical or enzymatic depolymerization, also bind CD44. However, it has been reported that a mixture of oligosaccharides with a degree of polymerization (DP) 4-20 exhibits pro-inflammatory effects, while HA polysaccharide exerts opposite effects (Gao, Yang, Mo, Liu, & He, 2008). This difference has been interpreted in terms of monovalent vs.

multivalent interactions. Clustering of CD44 would require multivalent HA-CD44 binding occurring with the HA polymer, whereas HA oligosaccharides could only allow monovalent interactions, thus preventing the receptor clustering. (Yang et al., 2012)

In this paper, we explore the use of small HA oligosaccharides of defined structure and purity. Our approach involved the chemical modification of these oligosaccharides (DP4, 6 and 8) and conjugation to a phospholipid moiety. These conjugates were used to prepare liposomes, which present at the surface a multivalent arrangement of these small oligosaccharides. After complete characterization of the liposomes, the cellular uptake by human lung cancer cells, the cell viability and the inflammatory profile were studied.

2. Materials and methods

2.1. Materials

Fetal bovine serum (FBS), fluorescein-5-(and-6)-sulfonic acid trisodium salts and culture medium were from Invitrogen Life Technologies (Carlsbad, CA). Plasticware for cell cultures was from Falcon (Becton Dickinson, Franklin Lakes, NJ). All the phospholipids were provided by Avanti Polar-Lipids distributed by Sigma-Chemical Co (St. Louis, MO). The protein content in cell extracts was assessed with the BCA kit from Sigma Chemical Co. Unless otherwise specified, all the other reagents were purchased from Sigma Chemical Co.

2.2. Analytical methods

^{1}H NMR (400 MHz) and ^{13}C NMR (101 MHz) spectra were recorded in D_2O. The proton and carbon signal assignments were determined from decoupling experiments. Thin layer chromatography (TLC) was performed on Silica F254 and detection by UV light at 254 nm or by charring with sulfuric acid in ethanol. High-resolution electrospray mass spectra in the positive ion mode were obtained on a Q-TOF Ultima Global hybrid quadrupole/time-of-flight instrument, equipped with a pneumatically assisted electrospray (Z-spray) ion source and an additional sprayer (Lock Spray) for the reference compound. The source

and desolvation temperatures were kept at 80 and 150 °C, respectively. Nitrogen was used as the drying and nebulizing gas at flow rates of 350 and 50 L/h, respectively. The capillary voltage was 3.5 kV, the cone voltage 100 V and the RF lens1 energy was optimized for each sample (40 V). Lock mass correction, using appropriate cluster ions of sodium iodide $(NaI)_nNa^+$, was applied for accurate mass measurements. The mass range was typically 50-2050 Da and spectra were recorded at 2 s/scan in the profile mode at a resolution of 10000 (FWMH).

2.3. Enzymatic hydrolysis of hyaluronic acid

Sodium hyaluronate (2 g) was dissolved in 0.1 M sodium acetate buffer (41 mL, pH 4.5) at 37 °C and bovine testes hyaluronidase (BTH, 12800 U) was added. After stirring for 2 days at 37 °C, 6000 U of enzyme were added. The addition of enzyme was repeated until TLC (n-butanol/formic acid/water, 2:2:1) showed no further changes (15 days). The solution was heated at 80°C for 5 min, filtered to remove the denatured enzyme, and freeze-dried. The crude product was desalted on Sephadex LH-20 using water as eluent. Analytical anion exchange chromatography (HPAEC) of the oligosaccharide mixture showed the presence of DP4, 6 and 8 as the main products.

2.4. Purification of oligosaccharides of DP4, DP6 and DP8 of hyaluronic acid

The separation of the oligosaccharides was performed on a HPLC Waters autopurification system (Waters, France) equipped with a 1525 binary pump coupled to a 2998 PDA detector (Waters, France), and a SEDEX LT-ELSD LC detector (Sedere, France). The run was performed at room temperature, the compounds were loaded on a TSKgel DEAE 5PW column (10 µm particle size, 200 mm x 50 mm) and the sample injection volume was 700 µl (aqueous solutions of compounds at 140 mg/mL). The mobile phase consisted of 1mM ammonium formate (solvent A) and 1M ammonium formate (solvent B). The composition of the mobile phase varied during the run as follows:

Condition prep: A:B: 0-20 min (100:0 to 85:15 v/v), 20-50 min (85:15 to 62:38 v/v), 50.01-60 min (0:100 v/v) at a flow rate of 30 mL/min.

Data acquisition and processing were performed with MassLynx V4.1 software.

After lyophilization, compounds **1a**, **1b** and **1c** were obtained in pure form in 14%, 16% and 17% yield, respectively.

2.5. Direct azidation of the oligohyaluronans of DP4, 6 and 8

Compounds **2a**-**c** were synthesized using a previously described methodology (Köhling et al., 2019). Briefly, 2-chloro-1,3-dimethylimidazolinium (DMC, 118 mg, 0.7 mmol) was added to a solution of oligohyaluronans (0.07 mmol), *N*-methylmorpholine (212 mg, 2.1 mmol) and NaN_3 (273 mg, 4.2 mmol) in water at 0 °C. The mixture was stirred at room temperature for 30 h and then was evaporated under reduce pressure. The 1-azidooligosaccharides **2a** and **2b** were purified on a Sephadex LH-20 column using deionized water to give the pure tetra- and hexasaccharide derivatives in 68% and 65% yield, respectively. The analytical data were in accordance to those previously reported (Köhling et al., 2019, 2016). The octasaccharide derivative was desalted using a Cellulose Ester (CE) dialysis membrane (MWCO: 100-500 Da) to afford **2c** (69 mg, 63% yield). ^{1}H NMR (D_2O, 400 MHz) δ 4.80 (1H), 4.50-4.47 (m, 3H), 4.44-4.40 (m, 4H), 3.94-3.71 (m, 24H), 3.63-3.51 (m, 12H), 3.40-3.32 (m, 4H), 2.04 (s, 3H, Ac), 2.03 (2s, 9H, Ac); ^{13}C NMR (D_2O, 101 MHz) δ 174.9 (*C*O), 103.0, 102.9, 100.7 (C-1), 88.5 (C-1 N_3), 82.9, 82.4, 81.9, 79.9, 77.4, 75.7, 75.5, 75.4, 75.3, 75.2, 73.6, 72.6, 72.3, 71.5, 68.4, 68.3, 60.5, 54.3, 54.2, 22.4; ESI-HRMS (positive ion): *m/z* [*M*+Na]$^+$ calcd for ($C_{56}H_{85}N_7O_{44}Na^+$): 1582.4527; found: 1582.4531.

2.6. General procedure for click reaction

DSPE-PEG(2000)-DBCO **3** (10 µmol) was dissolved in water (473 µL). An aqueous solution of the sugar residues (10 µmol in 190 µL of water) was added, the mixture was stirred at room temperature for 1 h and then was lyophilized. Compound **4a**: ESI-HRMS (neg.): *m/z*

130 [*M*-2H]$^{3-}$ calcd. for ($C_{179}H_{316}N_8O_{78}P^{3-}$): 1285.6888; found: 1285.6915. Compound **4b**: ESI-
131 HRMS (neg.): *m/z* [*M*-H]$^{2-}$ calcd. for ($C_{193}H_{338}N_9O_{89}P^{2-}$): 2118.5969; found: 2118.6045.
132 Compound **4c**: ESI-HRMS (neg.): *m/z* [*M*-2H]$^{3-}$ calcd. for ($C_{207}H_{358}N_{10}O_{100}P^{3-}$): 1538.4325;
133 found: 1538.4259.

134 *2.7. Liposomes preparation and characterization*

135 Liposomes were prepared by the thin lipid film hydration and extrusion method.
136 Chloroform solution of 1,2-distearoyl-*sn*-glycero-3-phosphocholine (DSPC), cholesterol
137 (CHOL) and 1,2-distearoyl-*sn*-glycero-phosphoethanolamine-N-[amino(polyethylene
138 glycol)-2000] (mPEG2000-DSPE) in a molar ratio 75:20:2 was mixed and evaporated under
139 reduce pressure to obtain a thin lipid film. The resulting lipid film was hydrated with a 20
140 mM 4-(2-hydroxyethyl)piperazine-1-ethanesulforic acid (HEPES) buffer (pH 7.4) and
141 vortexed for 10 min to obtain a suspension of multilamellar liposomes. The resulting
142 suspension was then extruded (Extruder, Lipex, Vancouver, Canada) 10 times under
143 nitrogen through 200 nm polycarbonate filter at 60°C.

144 To prepare decorated liposomes (LipoHA-DP4, LipoHA-DP6, LipoHA-DP8), the same
145 method was used. Lipid films were made up of DSPC/CHOL/mPEG2000-DSPE (75:20:2
146 molar ratio) and then hydrated using solution of the different HA-DP conjugates **4a**, **4b**
147 and **4c** (3 molar ratio) in HEPES buffer.

148 Fluorescently labeled liposomes were prepared as described above by adding 10 mM
149 solution of fluorescein-5-(and-6)-sulfonic acid trisodium salts in HEPES buffer during the
150 hydration of the lipid film. The unentrapped fluorescein was removed by gel filtration
151 using Sepharose® CL-4B column eluting with HEPES buffer. Liposomes were stored at 4 °C.

152 The mean particle size and polydispersity index (PI) of the liposomes were determined at
153 25 °C by quasi-elastic light scattering (QELS) using a nanosizer (Nanosizer Nano Z, Malvern
154 Inst., Malvern, UK). The selected angle was 173° and the measurement was made after

dilution of the liposomes suspension in MilliQ® water. Each measure was performed in triplicate.

The particle surface charge of liposomes was investigated by zeta potential measurements at 25 °C applying the Smoluchowski equation and using the Nanosizer Nano Z. Measurements were carried out in triplicate.

2.8. Cell cultures

Human epithelial lung cells BEAS-2B, human non-small cell lung cancer cells A549, NCI-H1385, NCI-H1975, NCI-H1650, NCI-H228, Calu-3 were purchased from ATCC (Manassas, VA). Cells were grown in RPMI-1640 medium, supplemented with 10% v/v FBS and 1% penicillin-streptomycin, at 37 °C, 5% CO_2, in a humidified atmosphere.

2.9. Flow cytometry

1×10^6 cells were rinsed and fixed with 2% w/v paraformaldehyde (PFA) for 2 min, washed three times with PBS and stained with the anti-CD44 antibody (Abcam, Cambridge, UK) for 1 h on ice, followed by an AlexaFluor 488-conjugated secondary antibody (Millipore, Burlington, MA) for 30 min. 1×10^5 cells were analyzed with EasyCyte Guava™ flow cytometer (Millipore), equipped with the InCyte software (Millipore). Control experiments included incubation with non-immune isotype antibody.

2.10. Cellular uptake

1×10^5 cells were seeded into a 96-well black plate, let to adhere for 6 h and incubated at different time points with the fluorescently labeled liposomes as indicated in the Results section. Cells were washed twice with PBS and rinsed with 300 µl PBS. The intracellular fluorescence, an index of liposome uptake, was measured using a Synergy HT Microplate Reader (Bio-Tek Instruments, Winooski, VT), using λ excitation 460 nm and λ emission 530 nm. Cells were then detached with tryspin/EDTA, sonicated and used for the measure of

intracellular protein contents. Results were expressed as fluorescence units (FU)/mg cellular proteins.

2.11. Cell viability

1×10^4 cells were seeded into a 96-well white plate, let to adhere for 6 h and incubated for 72 h with the liposomes as indicated in the Results section. Cell viability was measured by the ATPlite Luminescence Assay System (PerkinElmer, Waltham, MA), as per manufacturer's instructions. Results were analyzed by a Synergy HT Microplate Reader. The luminescence units of the untreated cells were considered 100%; the luminescence units of the other experimental conditions were expressed as percentage versus untreated cells.

2.12. Cytokine measurement

1 ml of cell culture supernatant was collected after 24 h treatment and probed with the Human Inflammation Antibody Array – Membrane (Abcam), as per manufacturer's instructions. Results were quantified by densitometry analysis of each dot blot, using Image J software (www.imagej.nih.gov). The dot blot density of untreated cells was considered 1; results of the treatment conditions were expressed as fold change (density of dot blot for each experimental condition/density of dot blot in untreated cells for the same cytokine).

2.13. Statistical analysis

All data in the text and figures are provided as means ± SD. The results were analyzed by a one-way analysis of variance (ANOVA) and Tukey's test. $p < 0.05$ was considered significant.

3. Results and discussion

3.1. Enzymatic treatment of hyaluronate and purification of hyaluronic oligosaccharides

Sodium hyaluronate (HA) was incubated with bovine testes hyaluronidase (BTH), an enzyme known for degrading HA to oligosaccharides. As BTH does not accept tetrasaccharides as substrates (Mahoney, Aplin, Calabro, Hascall, & Day, 2001) extensive enzymatic hydrolysis lead to the DP4 as the main product. We managed the reaction conditions in order to obtain a mixture of oligosaccharides.

A preparative HPAEC-ELSD was used to purify the oligosaccharides, using a DEAE-cellulose column and a gradient of aqueous solution of ammonium formate from 1mM to 1M as eluent. The main compounds of the mixture were eluted at 23.7 (DP4, **1a**), 28.6 (DP6, **1b**) and 32.7 min (DP8, **1c**) (Figure S1). After lyophilization, they were obtained in 14%, 16% and 17% yield, respectively. The analytical data of these oligosaccharides were in accordance with previous reported data (Blundell, Reed, & Almond, 2006; Tawada et al., 2002) (Figures S3-S5 and Table S1).

3.2. Synthesis of the phospholipo-oligohyaluronates

In order to study the impact of the length of the sugar residue in the liposomes, the oligohyaluronans were modified to perform the synthesis of the amphiphilic compounds. As shown in Scheme 1, a direct azidation of anomeric position was performed with 2-chloro-1,3-dimethylimidazolinium (DMC), *N*-methylmorpholine and NaN_3 in water at 0 °C. Compounds **2a**, **2b** and **2c** were obtained in 68%, 65% and 63% yield, respectively. ^{13}C NMR spectra of compounds **2a**, **2b** and **2c** showed the diagnostic signal at 88.5 ppm corresponding to the C1-N_3 (Figure 1).

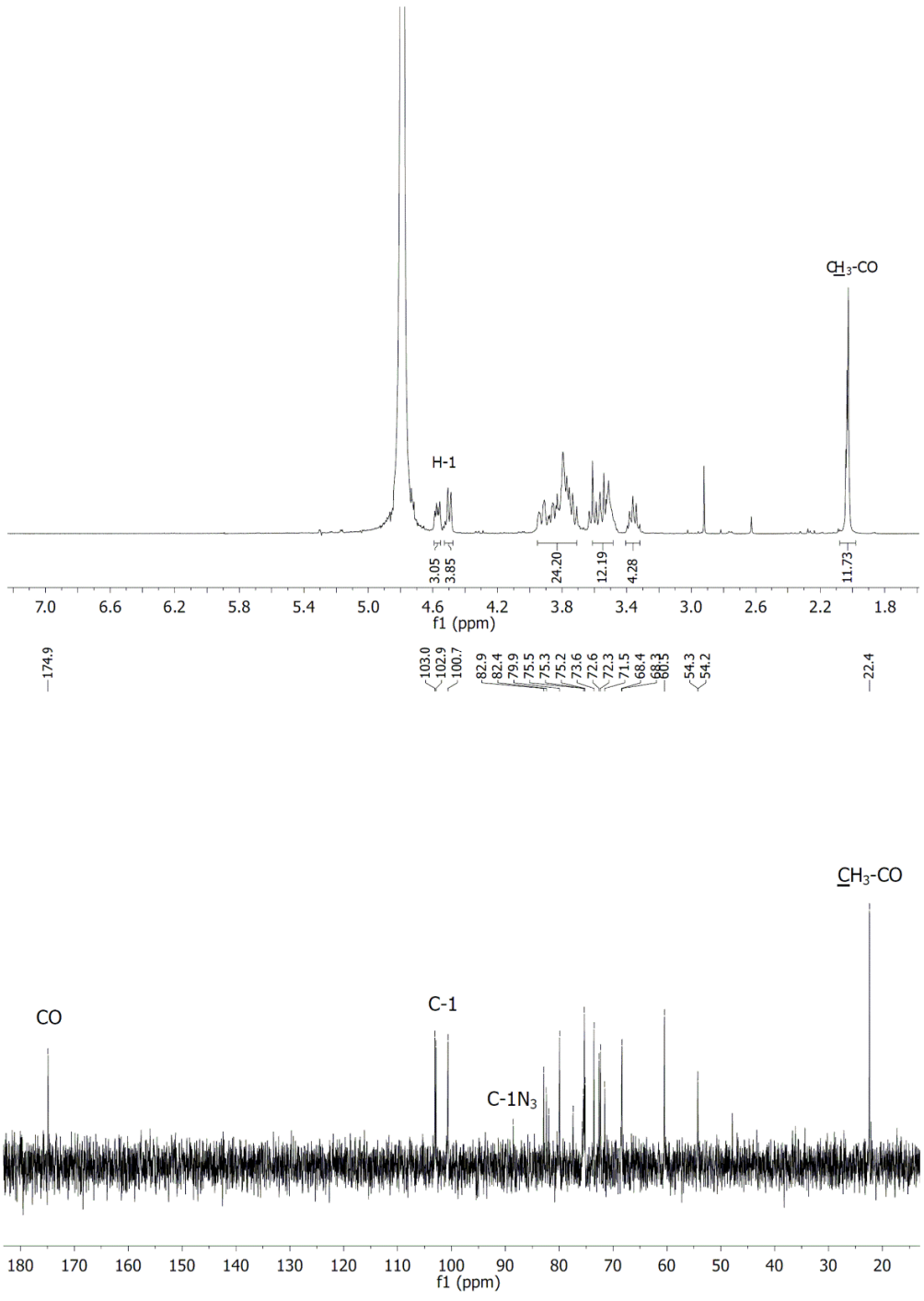

223

224 **Figure 1.** ^{1}H NMR (400 MHz) (top) and ^{13}C NMR (101 MHz) (bottom) spectra of compound

225 **2c** recorded in D_2O in a Bruker DRX 400.

Compounds **4a**, **4b** and **4c** were obtained by click reaction with DSPE-PEG(2000)-DBCO (**3**). This azadibenzocyclooctyne reacted spontaneously with the corresponding azidohyaluronate derivatives in water without addition of any catalyst, leading quantitatively to phospholipo-oligosaccharides **4a**, **4b** and **4c**. These compounds were characterized by ESI-HRMS. The spectra showed typical Gaussian profiles for the multi charged ions with *m/z* values that correspond to the products.

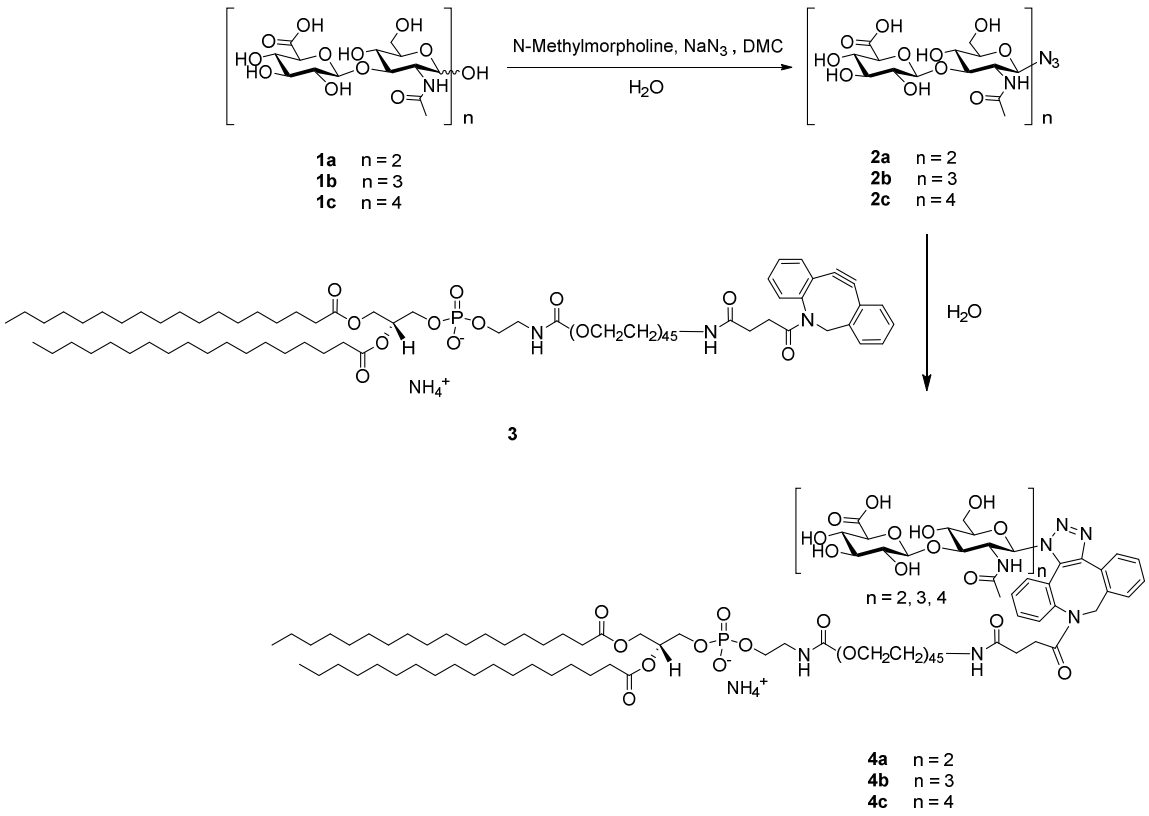

Scheme 1. Synthesis of phospholipo-oligohyaluronates.

3.3. Preparation and characterization of liposomes

Several papers report the preparation of HA decorated liposomes for the effective delivery of drug to CD44-expressing cells (Dosio, Arpicco, Stella, & Fattal, 2016); basically, two main approaches to insert HA into liposomes have been developed. In the first, HA is

linked to the surface of preformed liposomes by covalent conjugation between the carboxylic residues of HA and phospholipid amine groups (Yerushalmi, Arad, & Margalit, 1994). This method offers the advantage to conjugate HA only on the external surface of the particle but makes difficult the control the density of attachment of HA on the liposomes. In the second method HA oligomers are previously conjugated to a lipid anchor permitting the introduction of the conjugate into the lipid mixture during liposomes preparation in a controlled amount (Arpicco et al., 2013; Eliaz & Szoka, 2001; Marengo et al., 2019; Ruhela, Kivima, & Szoka, 2014).

To the best of our knowledge our compounds are the first examples of conjugates composed of HA oligomers linked to PEG phospholipids. The presence of PEG should improve the targeting ability of the systems decreasing the steric hindrance of the liposomes in the ligand-receptor interaction.

The HA-DP4 (**4a**), HA-DP6 (**4b**) and HA-DP8 (**4c**) conjugates were added at a molar ratio of 3 during hydration to a lipid film composed of DSPC/CHOL/mPEG2000-DSPE (75:20:2 molar ratio). In this way, the phospholipidic chain was completely incorporated into the liposome membrane, while the HA was exposed toward the aqueous phase; for comparison plain liposomes were prepared without adding the conjugates. The physicochemical characteristics of the different formulations are summarized in Table 1. Liposomes displayed a dimensional range of about 160 nm and the polydispersity index was low for all the formulations (< 0.18). Liposomes showed a negative Zeta potential value that was lower for decorated liposomes compared to plain ones, due to the carboxylic negative residues of conjugates. In particular, the negative charge slightly increased as the conjugate MW increased confirming the presence of glycoconjugates on the surface of the liposomes.

Table 1

Characteristics of plain and decorated liposomes. Values are the means ± SEM of three independent experiments each performed in triplicate.

Phospholipid composition	Mean particle size (nm)	Polydispersivity index	Zeta potential (mV)
PLAIN DSPC/Chol/mPEG-DSPE 75:20:2	163 ± 1.3	0.115	-9.3 ± 0.8
HA-DP4 DSPC/Chol/mPEG-DSPE/**4a** 75:20:2:3	166 ± 1.5	0.175	-27.1 ± 1.1
HA-DP6 DSPC/Chol/mPEG-DSPE/**4b** 75:20:2:3	165 ± 1.8	0.166	-32.6 ± 1.9
HA-DP8 DSPC/Chol/mPEG-DSPE/**4c** 75:20:2:3	166 ± 1.6	0.149	-35.3 ± 2.1
HA-4800 DSPC/Chol/mPEG-DSPE/HA-4800 75:20:2:3	176 ± 2.1	0.121	-19.3 ± 1.6
HA-14800 DSPC/Chol/mPEG-DSPE/HA-1480075:20:2:3	195 ± 2.4	0.175	-20.7 ± 1.4

3.4. Cellular uptake, viability and inflammatory profile

3.4.1 Cellular uptake

We preliminary screened different human non-small cell lung cancer cell lines for their expression of CD44, the receptor of HA, in comparison with non-transformed epithelial lung cells BEAS-2B. While CD44 was poorly expressed in BEAS-2B cells, in the cancer cell lines analyzed we detected cells with high (A549, NCI-H1650), moderate (NCI-H1975, Calu-3) and low CD44 expression (NCI-H1385, NCI-H228) (Figure S2).

With the aim of understanding the significance of oligomer length for receptor binding, we next evaluated the cellular uptake of the liposomes, by using fluorescently labelled particles and measuring the intracellular accumulation of the fluorophore. All cell lines displayed a dose-dependent uptake of the liposome cargo. In line with the different expression of CD44, the uptake of HA-DP4, HA-DP6 and HA-DP8-decorated liposomes was significantly higher in A549 and NCI-H1650 cells, and – to a lesser extent – in NCI-H1975 and Calu-3 cell, compared to plain liposomes. No differences in the uptake between

decorated and plain liposomes were detected in poorly expressing NCI-H1385 and NCI-H228 cells (Figure 2). This experimental set suggests that the entry of HA-conjugated formulations is likely receptor-mediated. Our hypothesis was confirmed by competition assays performed on CD44^{high} A549 and NCI-H1650 cells, incubated at different time points with liposomes in the presence of a saturating amount of anti-CD44 antibody or HA. As expected, the uptake increased over the time; such increase was higher with HA-decorated liposomes than with plain liposomes. However, the presence of anti-CD44 antibody or HA blunted the uptake of HA-decorated liposomes (Figure 3).

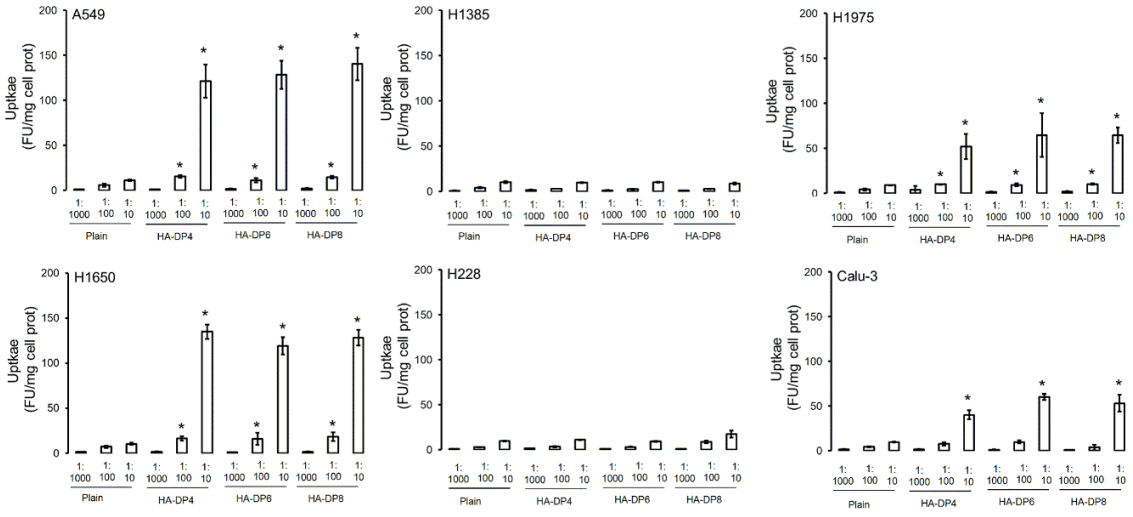

Figure 2. Cellular uptake of fluorescently labeled liposomes. A549, NCI-H1385, NCI-H1975, NCI-H1650, NCI-H228, Calu-3 cells were incubated 24 h with fluorescently labelled plain liposomes, HA-DP4-decorated, HA-DP6-decorated, HA-DP8-decorated liposomes, at a final dilution in the culture medium of 1:10, 1:100, 1:1000. The intracellular content of fluorescein, considered an index of liposome uptake, was measured spectrofluorimetrically in triplicates. Data are means ± SD (n = 4). * $p < 0.05$: HA-conjugated liposomes vs. corresponding plain liposomes.

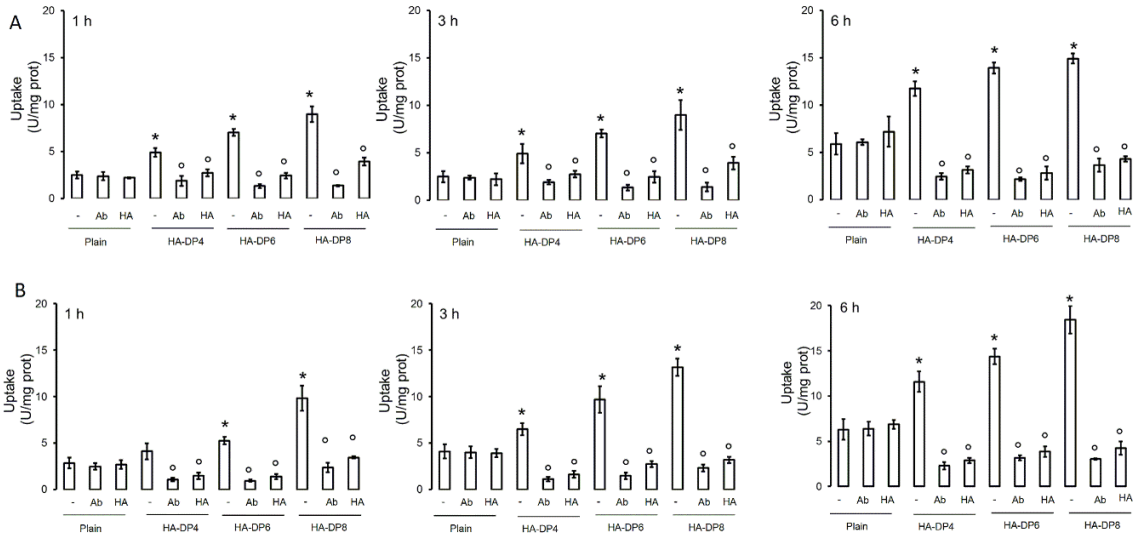

Figure 3. Competition assays in cellular uptake of fluorescently labeled liposomes. A549 (panel A) and NCI-H1650 (panel B) cells were incubated 1, 3 and 6 h with fluorescently labelled plain liposomes, HA-DP4-decorated, HA-DP6-decorated, HA-DP8-decorated liposomes, at a final dilution in the culture medium of 1:100, in the absence (-) or in the presence of an anti-CD44 antibody (Ab, at a final dilution of 1:10) or HA (100 μM). The intracellular content of fluorescein, considered an index of liposome uptake, was measured spectrofluorimetrically in triplicates. Data are means ± SD (n = 4). * $p < 0.05$: conjugated liposomes vs. corresponding plain liposomes; ° $p < 0.001$: Ab-HA-treated samples vs untreated (-) samples.

Interestingly, the amount of liposomes uptake at each time point followed this rank order: HA-DP8>HA-DP6>HA-DP4 liposomes at 1, 3 and 6 h (Figure 3), suggesting that the HA-DP8 formulations were optimal in inducing a fast receptor binding and triggering a receptor-mediated endocytosis.

To better compare the kinetics of entry of the liposomes with the structure of the conjugates used for their decoration, we analyzed the time-dependent uptake of liposomes prepared using conjugates previously synthetized in our laboratory (Arpicco et al., 2013) obtained by linking HA with two different molecular weight (4800 and 14800 Da)

to an aminated phospholipid by reductive amination. For this purpose, we used the highly CD44-expressing A459 cells and the poorly CD44-expressing NCI-H228 cells. While in the latter cell lines, there was always a lower uptake that did not change upon the time nor in presence of an excess of HA, in A549 cells we observed that HA-4800 conjugates were more taken up than HA-14800 conjugates at early time-points (1, 3 and 6 h). The difference was not maintained at 24 h. After 3, 6 and 24 h, the uptake was drastically reduced by HA in A549 cells, confirming that the intracellular delivery was CD44-dependent (Figure 4).

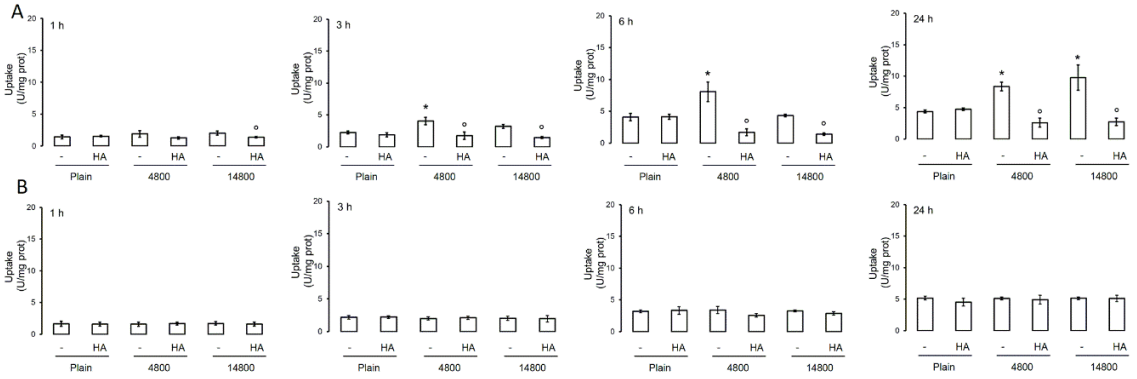

Figure 4. Competition assays in cellular uptake of fluorescently labeled liposomes with high and low molecular weight HA. A549 (panel A) and NCI-H228 (panel B) cells were incubated 1, 3, 6 and 24 h with fluorescently labelled plain liposomes, HA 4800 and HA 14800 liposomes, at a final dilution in the culture medium of 1:100, in the absence (-) or in the presence of HA (100 µM). The intracellular content of fluorescein, considered an index of liposome uptake, was measured spectrofluorimetrically in triplicates. Data are means ± SD (n = 4). * $p < 0.05$: conjugated liposomes vs. corresponding plain liposomes; ° $p < 0.05$: HA-treated samples vs untreated (-) samples.

This trend likely suggests that HA-DP4, 6 and 8 conjugates are capable of a faster interaction with CD44, followed by phagocytosis, while the entry of the other HA-conjugated liposomes requires more time. The sterical hindrance that makes the HA/CD44 interaction more complex and/or the need of CD44 clusterization upon the binding of

higher molecular weight HA conjugates may explain this difference. The presence of a PEG chain between the phospholipid and the HA oligomer in our conjugates should also improve the uptake. Moreover, at the same time point and in the same cell line, *i.e*. in the presence of the same amount of CD44, the uptake of both 4,800-HA and 14,800-HA conjugates was lower than the uptake of HA-DP4, the less effective conjugate in cellular delivery (Figure 2, 3 and 4).

3.4.2. Cell viability and inflammatory profile

We finally analyzed the biocompatibility of our formulations. After 72 h incubation, either unconjugated or HA-conjugated liposomes did not significantly reduce cell viability, in both $CD44^{low}$ and $CD44^{high}$ cells (Figure 5). In parallel, none of the formulations changed the expression of pro-inflammatory cytokines more than two-fold compared to untreated cells (Figure 6). These two results suggest that in our experimental conditions the liposomes are not cytotoxic and do not increase the release of potentially pro-inflammatory mediators. DP4-20 have pro-inflammatory properties in biological systems (Gao et al., 2008) and this side-effect may strongly limit the potential therapeutic application of HA-conjugates. Our results suggest the safety – in terms of lack of cytotoxicity and inflammatory effects – of HA-DP4, HA-DP6 and HA-DP8-liposomes, opening the perspective of their employment in nanomedicine.

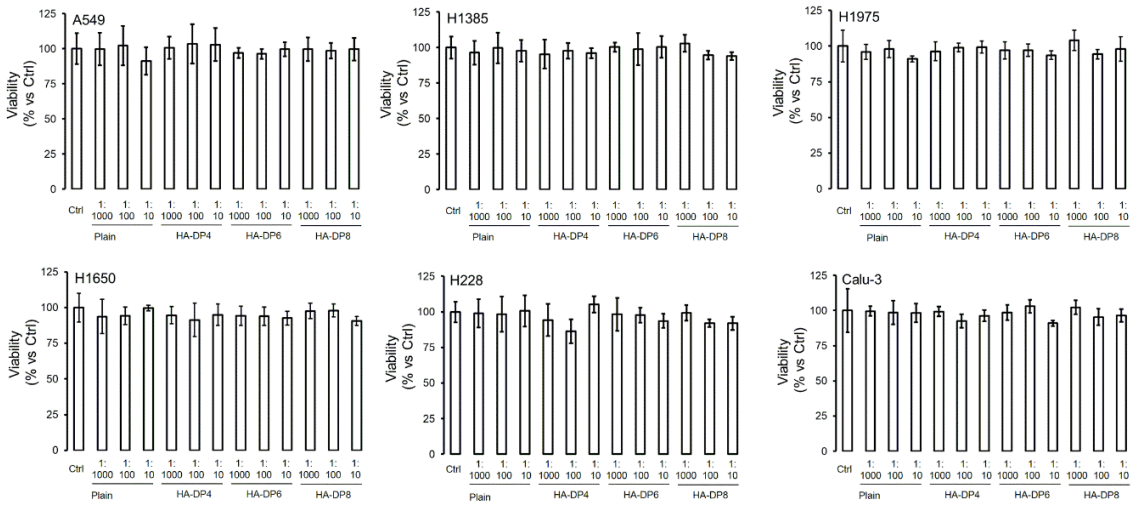

Figure 5. Viability of cells treated with liposomes. A549, NCI-H1385, NCI-H1975, NCI-H1650, NCI-H228, Calu-3 cells were incubated 72 h with fresh medium (Ctrl) or with medium containing plain liposomes, HA-DP4-decorated, HA-DP6-decorated, HA-DP8-decorated liposomes, at a final dilution in the culture medium of 1:10, 1:100, 1:1000. Cell viability was measured by a chemiluminescence-based assay in quadruplicates. Data are means ± SD (n =4).

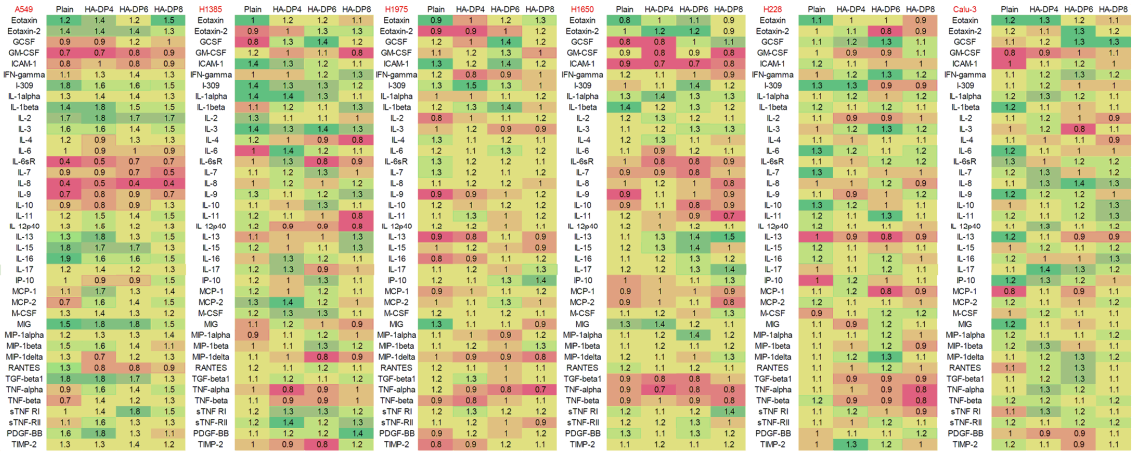

Figure 6. Cytokine production from cells treated with liposomes. A549, NCI-H1385, NCI-H1975, NCI-H1650, NCI-H228, Calu-3 were incubated 72 h with fresh medium (Ctrl) or with medium containing plain liposomes, HA-DP4-decorated, HA-DP6-decorated, HA-DP8-decorated liposomes, at a final dilution of 1:10. 1 ml of the culture medium was subjected to the detection of cytokines by antibody arrays. The dot blot density of untreated cells was considered 1; results of the treatment conditions were expressed as fold change (density of dot blot for each experimental condition/density of dot blot in untreated cells for the same cytokine), using a heatmap.

Indeed, exploiting the abundance of CD44 in non-small cell lung cancers (Chen, Zhao, Karnad, & Freeman, 2018; Penno et al., 1994), HA decorated liposomes can be used for the active targeting of anti-cancer drugs. Resistance to conventional chemotherapeutic agents (Chang, 2011) or targeted-therapies used in specific patients subsets with oncogenic mutations (Leonetti et al., 2018) is still a challenge in the therapeutic approach

of non-small cell lung cancers. The active targeting of tumors using anti-cancer drugs encapsulated in liposomes is more effective that the administration of free drugs against drug resistant tumors (Nag & Delehanty, 2019). This approach can improve in particular the efficacy and pharmacokinetic profile of first-line drug in non-small cell lung cancers such as cisplatin (Zhong et al., 2020). After evaluating the technical feasibility and binding of our conjugates, we are next planning to load suitable anti-cancer drugs, deeply characterize the formulations and evaluate their safety and anti-tumor efficacy against CD44-expressing non-small cell lung cancers.

4. Conclusions

Novel conjugates between HA oligomers of different DP (4, 6 and 8) and PEGylated phospholipid were prepared via click chemistry of 1-azido oligohyaluronates and azadibenzocyclooctyne phospholipid. These conjugates were introduced during the preparation of liposomes that were characterized in terms of size and zeta potential.

In order to evaluate their targeting *in vitro* studies on lung cancer cell lines with different expression of CD44 were done, to assess the ability of cellular delivery and the lack of toxicity or pro-inflammatory effects. This study is a proof of concept of the feasibility and biocompatibility of HA-conjugates, and opens the way to their future development as active-targeting agents carrying anti-tumor drugs.

Supplementary material

Purification of oligohyaluronates, surface expression of CD44 in lung cells and NMR spectra and HRMS of compounds **1a**, **1b** and **1c**.

Acknowledgments

This work was supported by the Centre National de la Recherche Scientifique (CNRS), l'Université de Picardie Jules Verne, the Agence Nationale de la Recherche (ANR-18-SUS2-

0001, France) and by the Italian Ministry for University and Research (MIUR)—University of Torino, “Fondi Ricerca Locale (ex-60%)”

References

Arpicco, S., Lerda, C., Dalla Pozza, E., Costanzo, C., Tsapis, N., Stella, B., … Palmieri, M. (2013). Hyaluronic acid-coated liposomes for active targeting of gemcitabine. *European Journal of Pharmaceutics and Biopharmaceutics*, *85*(3 Part A), 373–380. https://doi.org/10.1016/j.ejpb.2013.06.003

Blundell, C. D., Reed, M. A. C., & Almond, A. (2006). Complete assignment of hyaluronan oligosaccharides up to hexasaccharides. *Carbohydrate Research*, *341*(17), 2803–2815. https://doi.org/10.1016/j.carres.2006.09.023

Chang, A. (2011). Lung Cancer Chemotherapy, chemoresistance and the changing treatment landscape for NSCLC. *Lung Cancer*, *71*(1), 3–10. https://doi.org/10.1016/j.lungcan.2010.08.022

Chen, C., Zhao, S., Karnad, A., & Freeman, J. W. (2018). The biology and role of CD44 in cancer progression : therapeutic implications. *Journal of Hematology & Oncology*, *11*(64), 1–23. https://doi.org/10.1186/s13045-018-0605-5

Dalla Pozza, E., Lerda, C., Costanzo, C., Donadelli, M., Dando, I., Zoratti, E., … Palmieri, M. (2013). Targeting gemcitabine containing liposomes to CD44 expressing pancreatic adenocarcinoma cells causes an increase in the antitumoral activity. *BBA - Biomembranes*, *1828*(5), 1396–1404. https://doi.org/10.1016/j.bbamem.2013.01.020

Dosio, F., Arpicco, S., Stella, B., & Fattal, E. (2016). Hyaluronic acid for anticancer drug and nucleic acid delivery. *Advanced Drug Delivery Reviews*, *97*, 204–236. https://doi.org/10.1016/j.addr.2015.11.011

Eliaz, R. E., & Szoka, F. C. (2001). Liposome-encapsulated Doxorubicin Targeted to CD44 : A Strategy to Kill CD44-overexpressing Tumor Cells. *Cancer Research*, *61*, 2592–2601.

Fuster, M. M., & Esko, J. D. (2005). THE SWEET AND SOUR OF CANCER : GLYCANS AS NOVEL THERAPEUTIC TARGETS. *Nature Reviews Cancer*, *5*, 526–542.

https://doi.org/10.1038/nrc1649

Gao, F., Yang, C. X., Mo, W., Liu, Y. W., & He, Y. Q. (2008). Hyaluronan oligosaccharides are potential stimulators to angiogenesis via RHAMM mediated signal pathway in wound healing. *Clinical and Investigative Medicine*, *31*(3), 106–116. https://doi.org/10.25011/cim.v31i3.3467

Gazzano, E., Buondonno, I., Marengo, A., Rolando, B., Chegaev, K., Kopecka, J., … Riganti, C. (2019). Hyaluronated liposomes containing H2S-releasing doxorubicin are effective against P-glycoprotein-positive / doxorubicin-resistant osteosarcoma cells and xenografts. *Cancer Letters*, *456*, 29–39. https://doi.org/10.1016/j.canlet.2019.04.029

Köhling, S., Blaszkiewicz, J., Ruiz-Gómez, G., Fernández-Bachiller, M. I., Lemmnitzer, K., Panitz, N., … Rademann, J. (2019). Syntheses of defined sulfated oligohyaluronans reveal structural effects, diversity and thermodynamics of GAG-protein binding. *Chemical Science*, *10*(3), 866–878. https://doi.org/10.1039/c8sc03649g

Köhling, S., Künze, G., Lemmnitzer, K., Bermudez, M., Wolber, G., Schiller, J., … Rademann, J. (2016). Chemoenzymatic Synthesis of Nonasulfated Tetrahyaluronan with a Paramagnetic Tag for Studying Its Complex with Interleukin-10. *Chemistry - A European Journal*, *22*(16), 5563–5574. https://doi.org/10.1002/chem.201504459

Leonetti, A., Assaraf, Y. G., Veltsista, D., El Hassouni, B., Tiseo, M., & Giovannetti, E. (2018). MicroRNAs as a drug resistance mechanism to targeted therapies in EGFR- mutated NSCLC: current implications and future directions. *Drug Resistance Updates*, *42*, 1–11. https://doi.org/10.1016/j.drup.2018.11.002

Mahoney, D. J., Aplin, R. T., Calabro, A., Hascall, V. C., & Day, A. J. (2001). Novel methods for the preparation and characterization of hyaluronan oligosaccharides of defined length. *Glycobiology*, *11*(12), 1025–1033. https://doi.org/10.1093/glycob/11.12.1025

Marengo, A., Forciniti, S., Dando, I., Dalla, E., Stella, B., Tsapis, N., … Palmieri, M. (2019). Pancreatic cancer stem cell proliferation is strongly inhibited by diethyldithiocarbamate- copper complex loaded into hyaluronic acid decorated liposomes Alessandro. *BBA - General Subjects*, *1863*(1), 61–72.

https://doi.org/10.1016/j.bbagen.2018.09.018

Nag, O. K., & Delehanty, J. B. (2019). Active Cellular and Subcellular Targeting of Nanoparticles for Drug Delivery. *Pharmaceutics*, *11*(10), 543–570. https://doi.org/10.3390/pharmaceutics11100543

Penno, M. B., August, J. T., Baylin, S. B., Mabry, M., Linnoila, R. I., Lee, V. S., … Rosada, C. (1994). Expression of CD44 in Human Lung Tumors. *Cancer Research*, *54*, 1381–1388.

Ruhela, D., Kivima, S., & Szoka, F. C. (2014). Chemoenzymatic Synthesis of Oligohyaluronan − Lipid Conjugates. *Bioconjugate Chemistry*, *25*, 718–723. https://doi.org/10.1021/bc4005975

Tawada, A., Masa, T., Oonuki, Y., Watanabe, A., Matsuzaki, Y., & Asari, A. (2002). Large-scale preparation, purification, and characterization of hyaluronan oligosaccharides from 4-mers to 52-mers. *Glycobiology*, *12*(7), 421–426. https://doi.org/10.1093/glycob/cwf048

Toole, B. P. (2004). HYALURONAN : FROM EXTRACELLULAR GLUE TO PERICELLULAR CUE. *Nature Reviews Cancer*, *4*, 528–539. https://doi.org/10.1038/nrc1391

Yang, C., Cao, M., Liu, H., He, Y., Xu, J., Du, Y., … Gao, F. (2012). The High and Low Molecular Weight Forms of Hyaluronan Have Distinct Effects on CD44 Clustering * □. *The Journal of Biological Chemistry*, *287*(51), 43094–43107. https://doi.org/10.1074/jbc.M112.349209

Yerushalmi, N., Arad, A., & Margalit, R. (1994). Molecular and Cellular Studies of Hyaluronic Acid-Modified Liposomes as Bioadhesive Carriers for Topical Drug Delivery in Wound Healing. *Archives of Biochemistry and Biophysics*, *313*(2), 267–273. https://doi.org/10.1006/abbi.1994.1387

Zhong, Y., Jia, C., Zhang, X., Liao, X., Yang, B., Cong, Y., … Gao, C. (2020). European Journal of Medicinal Chemistry Targeting drug delivery system for platinum (Ⅳ) -Based antitumor complexes. *European Journal of Medicinal Chemistry*, *194*, 112229. https://doi.org/10.1016/j.ejmech.2020.112229